V. Specific Parameter Values and the Resultant Device Characteristics

The phase shifter whose characteristics have been optimized according to the procedure described has the following parameter values:

1) a_0 = 0.900 inches.
2) $d/a_0 = 0.125$.
3) ϵ = 2.54.
4) L = 5.0 inches.
5) Δa vs w, Curve B, Fig. 3.

The above design more than meets the original specifications of 360° variable phase shift, ±5° maximum phase error, and 10 per cent bandwidth. Although no attempt was made to compensate for the discontinuities in this model, measurements made on a similar experimental model indicate that a one-half wavelength taper of the dielectric slab will result in a VSWR < 1.15 and an insertion loss < 0.5 db. In addition, the structure is small and rugged, and capable of handling several hundreds of watts peak power. Maintaining the proper relationship between wall and dielectric motion requires a somewhat complex drive and is not accomplished easily; however, the construction of a suitable drive mechanism is certainly feasible.

It is significant to compare these results with two other configurations. The first has the following parameter values:

1) a_0 = 0.900 inches.
2) $d/a_0 = 0.200$.
3) ϵ = 2.54.
4) L = 7.1 inches.
5) Δa = 0.

This configuration can be described simply as a dielectric-vane phase shifter. (This is the configuration of many commercially available phase shifters.) A length of 7.1 inches is needed to achieve 360° of variable phase shift because of the large initial phase shift. The phase error is 48° at this setting. TE_{20} mode excitation can also occur. Obviously these parameters cannot be employed in this application. A second possibility is

1) a_0 = 0.900 inches.
2) $d/a_0 = 0.100$.
3) ϵ = 2.54.
4) L = 6.8 inches.
5) Δa = 0.040.

The wall position is held fixed although displaced from its normal location. The obvious advantage of a fixed wall is mechanical simplicity. Over a 6 per cent bandwidth the maximum phase error is 6°. TE_{20} mode conversion does not take place. Although this configuration does not meet the original specification, it does hold promise where limited bandwidth operation is desired.

Acknowledgment

The authors wish to thank the following members of the IBM Research Staff: Mrs. E. Smith for her computer programming assistance and P. Lockwood, J. Parrish and J. Smith for their activities in the construction and measurement of experimental models.

We also wish to thank W. Summers of IBM Federal Systems Division, Owego, N. Y., for his support and encouragement of this activity.

In addition, we wish to acknowledge the assistance of Prof. A. A. Oliner in his capacity as consultant to the project.

A New Technique for Multimode Power Measurement*

JESSE J. TAUB†, SENIOR MEMBER, IRE

Summary—**A new and simple technique for measuring total power flow to within ±1 db in an overmoded waveguide has been developed. A set of fixed probes (typically, 40 probes) samples the electric fields normal to the surface of an enlarged waveguide section. The enlarged waveguide and a dispersive line stretcher permit quick determinations of power delivered to a matched load when the power is propagating in a large number of modes. Extension to the case of a mismatched load is also discussed. This technique is useful for measuring spurious emissions of microawave transmitters and power flow in millimeter and submillimeter waveguides.**

* Received May 7, 1962; revised manuscript received July 31, 1962.

† Department of Applied Electronics, Airborne Instruments Laboratory, a Division of Cutler-Hammer, Inc., Deer Park, N. Y.

I. Introduction

MOST DEVICES that can measure the power flowing within a microwave transmission line are designed on the basis of a single propagating mode—usually the TE_{10} mode in rectangular waveguide or the TEM mode in coaxial line. In recent years a need has arisen for a device that accurately measures the power flow over a wide range of power levels (−50 to +50 dbm or more) in a transmission line that has two or more propagating modes. This problem exists when measuring the power contained in the spurious outputs of a microwave transmitter. It also arises in overmoded

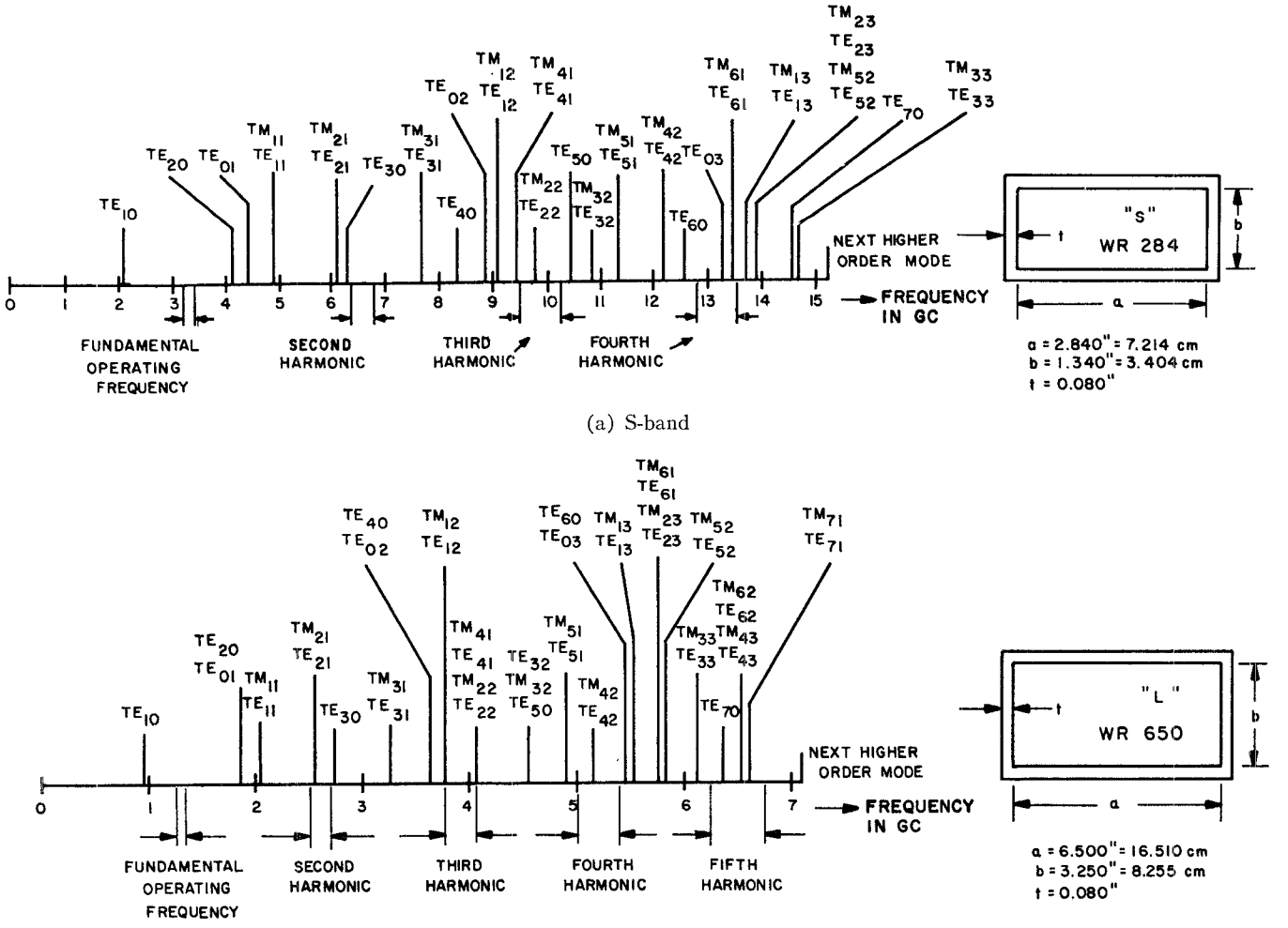

(a) S-band

(b) L-band

Fig. 1—Mode cutoff frequencies in *S*-band and *L*-band rectangular waveguides.

waveguides at millimeter wavelengths but over a smaller dynamic range.

If, for example, the third harmonic power from an *S*-band magnetron is to be measured, it is found that the waveguide can support the TE_{10} (dominant mode) plus 15 higher modes [(Fig. 1(a)]; if the measurement of a fifth harmonic is desired, one must contend with over 35 higher modes [(Fig. 1(b)]. This indicates that conventional techniques such as bolometers and calibrated crystals are inadequate with such complex field distributions. Multimode water loads and other calorimetric techniques do not have adequate sensitivity in the −50 dbm region.

Techniques for measuring the power flow in a multimode transmission line have been previously developed by Forrer and Tomiyasu, Price, Lewis, and Sharp and Jones [1], [2], [3], and [4].

Forrer and Tomiyasu built a moving-probe assembly that could measure the magnitude and phase of the electric field at the walls of a standard size rectangular waveguide. By performing a Fourier analysis on these measured values, they were able to calculate the power flow in each propagating mode. The total spurious-emission power at the frequency of interest was calculated by summing the power in each mode. The method is sound, but a digital computer is required to reduce the data and the sliding probe was subject to voltage breakdown under high power conditions. To avoid arcing, the higher power source was turned off each time the probe was moved—a possible source of error because it could not be known whether the power output or the modal content was the same when the high power source was turned on again.

Price developed a fixed-probe method that measured the electric fields normal to the waveguide walls. The modal amplitude was then calculated with the aid of a digital computer (in a manner similar to that used by Forrer and Tomiyasu). The fixed-probe method was arc-free, but like the moving-probe method it had the disadvantage of requiring a computer. Each power measurement required several minutes for data reduction.

Lewis developed a mode coupling method in which a series of mode couplers selectively couples a given mode to its own output port. By calibrating the mode couplers, it is possible to measure the total spurious-emission power by summing the power at each output port. This method has merit if the power is concentrated in a

known limited number of modes. This requirement is a definite restriction on its usefulness.

Sharp and Jones developed a sampling technique for regular size waveguides that is useful for rapidly sorting out harmonic power into many single-mode waveguides. This approach does not require a computer. The measurement accuracy is, however, no better than ± 2 to ± 5 db.

The new technique described here uses a set of fixed probes in an oversize waveguide. Multimode power can be measured at any frequency within a few seconds and the measurement is accurate to ± 1 db. The oversize waveguide converts the energy to an approximate plane wave, which simplifies the measurement. The oversize waveguide also improves the power-handling capability by a factor of 9 over conventional techniques. Power measurements can be made readily both at high power levels (higher than 10 Mw and S-band) and at low power levels (as low as -50 dbm).

This paper presents the theoretical basis for the measurements together with experimental verification and a brief description of the equipment used. (For additional information on this equipment, see [5].)

II. Power Measurement into a Matched Load

The multimode power propagating down a waveguide terminated in a load matched for all modes is measured using the equipment shown in Fig. 2. It consists of a variable length of standard size waveguide (line stretcher), a tapered section for connecting the input waveguide to a section of oversize waveguide, a set of fixed probes (usually 30 to 40) sampling the field normal to the walls of the oversize waveguide, and a multimode load. The probes are coupled to a switching assembly that couples each probe sequentially to the common receiver.

Initial measurements were made with a series of manually operated coaxial switches (Fig. 3). An automated version using a microwave commutator is under development. The commutator sequentially switches each of the 36 probe outputs to the common receiver. With the aid of this device, complete probe averaging can be completed in less than 30 sec.

The line stretcher varies the time phases of the propagating modes relative to each other. The taper must be able to transfer all the power to the oversize waveguide and not generate any new modes of its own. It was found that this could best be done using a cosine^2 taper of the type described by Unger [6] and Tang [7]. A 3-ft taper (Fig. 4) connecting an S-band (1.5 in $\times$3 in) waveguide to the oversize (5.8 in$\times$8.5 in) waveguide was experimentally found to have negligible mode conversion. The tapering of the oversize guide launches a plane wave—a situation necessary for achieving direct power averaging.

The electric field is sampled by a set of boundary probes; a fixed-probe section is shown on the left of Fig. 3. Each probe is decoupled from the waveguide by at least 40 db to minimize mode conversion effects due

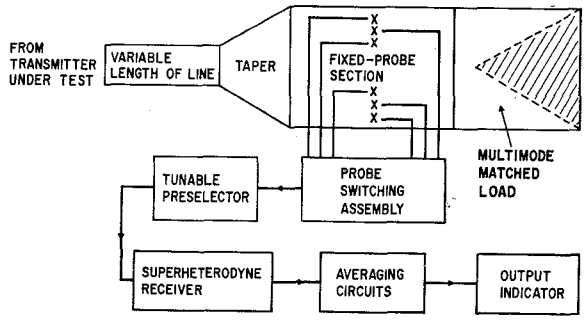

Fig. 2—Block diagram of equipment for fixed-probe technique.

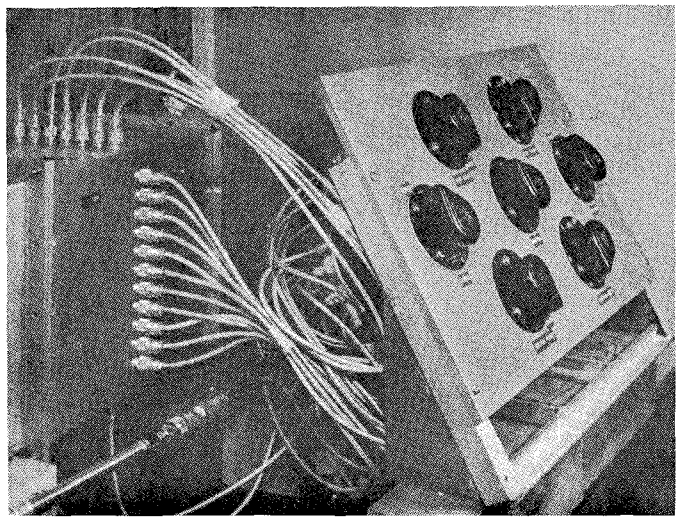

Fig. 3—Probe-switching assembly.

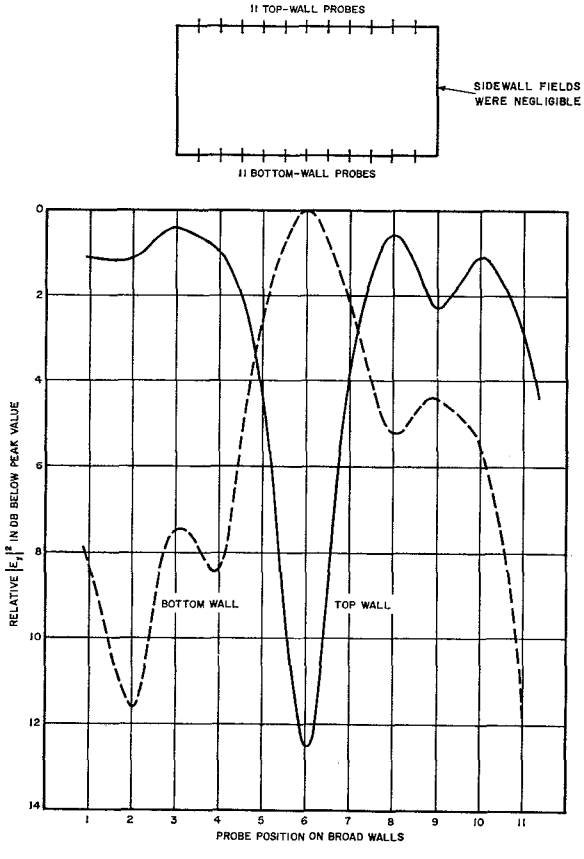

Fig. 4—Field distribution for multimode power measurement.

to the probes. The multimode power flow in the waveguide is then determined by the relationship

$$P = \frac{ab}{2\eta\delta}\left[\frac{1}{K}\sum_{k=1}^{K} |E_{yk}|^2 + \frac{1}{L}\sum_{l=1}^{L} |E_{xl}|^2\right] \quad (1)$$

where

a = the length of the broad wall of the enlarged waveguide,
b = the length of the narrow wall of the enlarged waveguide,
η = the intrinsic impedance of free space = 120π ohms,
K = the number of broad wall probes,
L = the number of narrow wall probes,
$|E_{yk}|^2$ = the squared magnitude of rms electric field normal to a broad wall at the kth probe,
$|E_{xl}|$ = the squared magnitude of rms electric field normal to a narrow wall at the lth probe,
δ = a constant that varies from 0.5 to 1 depending on the modal content.

This expression is derived in Appendix I. The power is determined from knowledge of the average value of $|E|^2$ at the boundary of the waveguide. This average is obtained by sampling the probe outputs with a superheterodyne receiver whose output current is proportional to $|E|^2$. The outputs are fed to a common receiver by means of an RF switching arrangement.

The main source of error is the choice of δ. There can be as much as a ± 1.5-db error because of this uncertainty but, as pointed out in Appedix I, for most cases a δ value of 0.612 would result in a maximum error of ± 0.88 db.

Section III and Appendix I also show that this averaging technique is in error because of a set of terms caused by cross products of higher mode fields. This can be expressed.

$$P_a = P_T + \text{error terms}$$

where P_T is the true power flow into a matched load or

$$P_a = P_T + \frac{ab}{8\eta}\sum_{m=0}^{M}\left\{\sum_{n_2=0}^{N}\sum_{\substack{n_1=0 \\ n_1 \neq n_2}}^{N} E_{mn_1}E_{mn_2}^*[1 + (-1)^{n_1+n_2}]\right\}_y$$

$$+ \frac{ab}{8\eta}\sum_{n=0}^{N}\left\{\sum_{m_2=0}^{M}\sum_{\substack{m_1=0 \\ m_1 \neq m_2}}^{M} E_{m_1n}E_{m_2n}^*[1 + (-1)^{m_1+m_2}]\right\}. \quad (2)$$

The two cross-product terms refer to y and x field components respectively. The error terms are real quantities that can be positive or negative depending on the phases of $E_{mn_1}E_{mn_2}$* and $E_{mn_1}E_{m_2n}$*. This phase can be varied by changing the length of the line stretcher. If measurements of P_a are made at several lengths of the line stretcher, the true power flow P_T is determined by arithmetically averaging the values of P_a. If the line stretcher is set for maximum and minimum values of P_a, the true power is given, to a good approximation, by the arithmetic average of the two P_a readings. The P_a readings are obtained directly from an output indicator that is designed to average the readings obtained from each probe setting.

III. Experimental Results

Experimental verification of this technique has been obtained by launching multimode fields of known power levels and correlating them with fixed-probed measurements. This approach has been used to date for about 10 different multimode distributions. Good accuracy (less than ± 1−db error) has always been obtained. Fig. 4 shows a typical field distribution launched into the oversize waveguide. The measurement was made at 7 Gc with the wave launched in a standard S-band waveguide and then tapered to the enlarged waveguide fixed-probe section. The field was measured on all four walls. Only the $|E_y|$ components are plotted; the $|E_x|$ components were much lower and had only 0.2-db effect on the power calculation. The power resulting from this field distribution agreed with the true power reading within ± 0.9 db.

The power was computed from knowledge of the coupling coefficients of the fixed probes. These coefficients were determined by first launching a pure TE_{10} mode into the oversize waveguide and measuring the insertion loss (ratio of oversize waveguide available power to the power delivered to the load terminating each probe). The insertion loss is measured with each probe placed in the center of the broad face of the waveguide. The average value of all probe insertion losses (36 readings) defines a calibration constant, C_p (see Hinkelmann, *et al*, [8] for further details). The power in a general multimode field is then determined by averaging the power readings from all probes and multiplying by C_p. The final result was then obtained by averaging the maximum and minimum readings for different settings of the line strectcher.

The fixed-probe section was measured for peak power-handling capacity in the 2.7- to 2.9-Gc range. No evidence of breakdown was found for peak power levels as high as 3.5 Mw. It is believed that the device can operate (with the waveguide pressurized to 15 psig) at power levels as high as 10 Mw.

IV. Theoretical Considerations

A. General

The theoretical basis of the fixed-probe technique applies to any uniform transmission line. It is, however, discussed below for a rectangular waveguide.

B. Use of Enlarged Waveguide

The multimode field to be measured will, in general, contain some modes that are near cutoff and hence will propagate in a dispersive manner.

The power flow in this waveguide is derived in Appendix II. The result is

$$P = \int_0^b \int_0^a \mathrm{Re}\,(E_x H_y^* - E_y H_x^*)\,dx\,dy \qquad (3)$$

Examination of (3) indicates that the phase and rms magnitudes of E_x, E_y, H_x and H_y must be measured over the entire xy plane to obtain the data for performing the desired integration. The complexity of measuring the above eight quantities is considerably reduced by performing the measurement in enlarged waveguide. Appendix II shows that the power flow expression reduces to

$$P_T \approx \frac{1}{\eta} \int_0^b \int_0^a (|E_x|^2 + |E_y|^2)\,dx\,dy \qquad (4)$$

for a and b arbitrarily large.

Appendix II also shows that for a and b dimensions equal to three times that of the input waveguide, the maximum possible error in (4) is 6 per cent. The problem is therefore reduced to the measurement of two quantities $|E_x|^2$ and $|E_y|^2$ over the wave guide cross section.

Eq. (4) is used as the starting point in deriving (1) and (2) for the fixed-probe technique. This is discussed in the next paragraph.

C. Validity of Averaging Technique

Appendix I shows that the power measurement made by using fixed boundary probes yields the true power expression (4) plus error terms. The error terms are real quantities that can be positive or negative, depending on the relative time phases of the propagating modes. The error terms consist of cross products of field components of certain modes. A typical term from (2) is $|E_{01x}|\,|E_{21x}|\cos\,[\phi_1-(\beta_{21}-\beta_{01})l]$, which is a real quanity that can be either positive or negative. Many of the terms cancel when m_1+m_2 or n_1+n_2 are even numbers, tending to reduce the complexity. Although the error terms are functions of many of the modal amplitudes, in many cases most of the spurious power is carried in no more than four modes. This observation is based on examination of data taken at General Electric [9] (obtained by numerical harmonic analysis). If these data are typical, the error terms will be at most one or two quantities.

To eliminate this source of error, fixed-probe readings are taken several times; each time the phase relationships between the modes are shifted by using a waveguide line stretcher located in the small dispersive waveguide. The average of these readings will give a good approximation to the true power.

D. Examples

A better understanding of the error term problem can be obtained by considering some typical cases.

Appendix III derives the error in terms of the possible propagating modes for the case of a third-harmonic signal propagating in S-band (WR284) waveguide (Table I). The exact results are found in (35). Examination of typical transmitter-waveguide launching structures and the data shown in Section VI of Price, *et al.* [9] indicates that the elimination of modes having even m-indices is justified. We shall therefore apply the equations to a symmetrically fed waveguide (35).

Examination of these data indicates that the assumption of a center-fed transition is good. For this tube, the error term (36) reduces to

$$\mathcal{E}_y = 0$$

$$\mathcal{E}_x = \frac{ab}{2\eta}\,\mathrm{Re}\,(E_{11_x}E_{31_x}^*).$$

The $\mathcal{E}_x$ error, which from the above data is seen to be small, can be completely averaged out by permitting the phase of E_{11} to vary relative to E_{31} by using the previously mentioned dispersive waveguide line stretcher.

Ref. [9] also gives data for the fifth harmonic of two QK-358 magnetrons operating at a fundamental frequency of 1250 Mc. These data show that the fifth-harmonic power is concentrated in the same mode numbers for both tubes. Table II lists the modal power of one of these tubes and neglects all modes whose power is less than 0.2 per cent of the total fifth-harmonic power.

TABLE I
THIRD-HARMONIC POWER DISTRIBUTION (QK-338 MAGNETRON)**

Fundamental frequency:	2768.6 Mc
Third-harmonic frequency:	8305.7 Mc
Fundamental TE_{10}) power:	4.6 Mw
Third-harmonic power for each mode:	
TE_{10}	4285 w
TE_{20}	127 w
TE_{30}	9691 w
TE_{40}	—
TE_{01}	1 w
TE_{11}	36 w
TM_{11}	467 w
TE_{21}	26 w
TM_{21}	140 w
TE_{31}	260 w
TM_{31}	849 w

** Data taken from [9].

TABLE II
MODAL POWER DISTRIBUTION (QK-358 MAGNETRON)

TE Mode	Power (watts)	TM Mode	Power (watts)	Total Power per Mode Index (watts)
TE_{01}	9539	—	—	9539
TE_{02}	1501	—	—	1501
TE_{11}	8564	TM_{11}	2328	10,892
TE_{21}	981	TM_{21}	1176	2157
TE_{31}	56	TM_{31}	112	168
TE_{12}	1759	TM_{12}	143	1902

Although the fifth harmonic has over 25 errors terms [10] for the data shown above, $\mathcal{E}_y \approx 0$ and $\mathcal{E}_x$ reduces to only two terms

$$\mathcal{E}_x \approx \frac{ab}{2\eta} \operatorname{Re}\,(E_{01_x}E_{21_x}^* + E_{11_x}E_{31_x}^*).$$

The use of the dispersive line stretcher should average out this $\mathcal{E}_x$ term.

E. Frequency Limitations

The fixed-probe technique can accurately sample multimode power provided the highest mode index for both broad and narrow walls is no greater than the number of sampling probes [9]. For the particular fixed-probe section described in this paper, the limiting mode indices are $m=11$ and $n=7$. The maximum frequency would correspond to the cutoff frequency of the next higher mode—$m=12$ and $n=7$. This critical frequency is

$$f_c = \frac{c}{2}\left[\left(\frac{12}{a}\right)^2 + \left(\frac{7}{b}\right)^2\right]^{1/2}$$

where c is the velocity of light.

For S-band waveguide, $a=2.84$ in and $b=1.34$ in, f_c is 39.7 Gc, which is the thirteenth harmonic of an S-band frequency.

It is likely that other difficulties such as higher mode generation by the probes and mode purity in the coaxial lines connecting the probes to the receiver would limit the usefulness to a lower frequency. Furthermore, the error terms would be difficult to average because of the multiplicity of cross products [10]. It is estimated that the device, in its present form, is useful for frequencies as high as the seventh harmonic of the fundamental frequency.

V. Mismatched Loads

The discussion up to this point has assumed that measurements are made into matched loads. The fixed-probe technique can also be used to measure the power delivered to a mismatched load. The power delivered to a multimode mismatched load P_T is measured by

$$P_T = 2P_M - P_a \tag{5}$$

where

P_M = the power measured into a multimode matched load (discussed in Section II),

P_a = the power measured by the fixed probe averaging for all variations of a small waveguide line stretcher and either a large waveguide line stretcher or a set of three or more fixed-probe planes along the Z axis.

The large waveguide line stretcher or the sets of probes are located between the fixed-probe section and the load.

This result is obtained by carrying through an analysis similar to that of Appendix I with the E_x and E_y components (11) and (12) modified as follows:

$$E_x = \sum_{n=0}^{N}\sum_{m=0}^{M} E_{mn_x}[1 + \Gamma_{mn}\epsilon^{j2\beta_{mn}z}] \cos\frac{m\pi x}{a}\sin\frac{n\pi y}{b}$$

and

$$E_y = \sum_{n=0}^{N}\sum_{m=0}^{M} E_{mn_y}[1 + \Gamma_{mn}\epsilon^{j2\beta_{mn}z}] \sin\frac{m\pi x}{a}\cos\frac{n\pi y}{b} \tag{6}$$

where

Γ_{mn} = the reflection coefficient for the mn mode at $z=0$,

β_{mn} = the propagation constant for the mn mode.

Use of these more general field equations and noting that β_{mn} is, to a good approximation, equal to β_0 (the free space propagation constant) for all modes in the enlarged waveguide, results in a P_p term of

$$P_p = \frac{ab}{4\delta C\eta}\sum_{m=0}^{M}\sum_{n=0}^{N}(|E_{mn_x}|^2 + |E_{mn_y}|^2) \cdot[1 + |\Gamma_{mn}|^2 + 2|\Gamma_{mn}|\cos(2\beta_0 z - \psi_{mn})] \tag{7}$$

where ψ_{mn} is the phase associated with Γ_{mn}.

After varying the large waveguide line stretcher and taking the average value of P_p, we obtain

$$P_a = \frac{ab}{4\delta C\eta}\left\{\sum_{m=0}^{M}\sum_{n=0}^{N}(|E_{mn_x}|^2 + |E_{mn_y}|^2) + \sum_{m=0}^{M}\sum_{n=0}^{N}|\Gamma_{mn}|^2(|E_{mn_x}|^2 + |E_{mn_y}|^2\right\}. \tag{8}$$

The above expression can be expressed as

$$P_a = P_M + P_R. \tag{9}$$

We wish to measure the power absorbed by a mismatched termination, which is

$$P_T = P_M - P_R \quad \text{or} \quad P_R = P_T + P_M. \tag{10}$$

Subsitution of (10) in (9) gives the desired result (5).

Fig. 5 is a block diagram of equipment that can measure P_m and P_a. The device is similar to the one shown in Fig. 2, except for the addition of the phase variation of the load reflection coefficients. The load phase variation is created by sampling the electric fields at several xy planes in the large waveguide; four sampling planes are used. The use of discrete xy plane

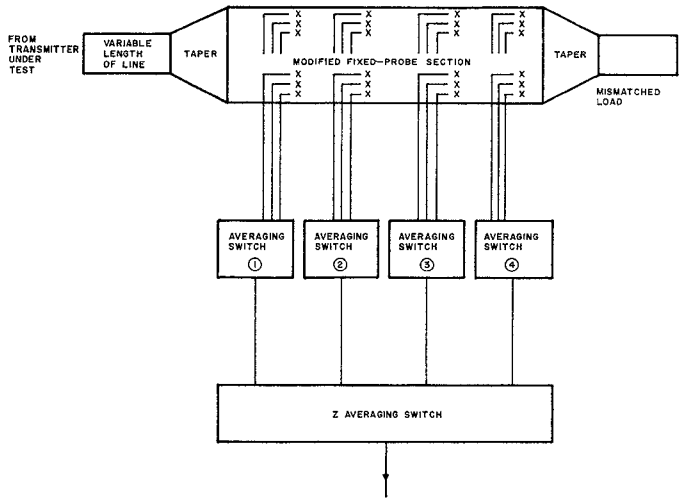

Fig. 5—Block diagram of equipment for fixed-probe technique modified for mismatched loads.

sampling is preferable to the oversize waveguide line stretcher because it lends itself more easily to automatic measurements. This averaging can be done automatically by means of the commutators shown in the block diagram.

There may be some applications where it is not convenient to measure P_M as well as P_a. The value of P_a can be in error by twice the reflected power. This is shown by subtracting (10) from (9) giving

$$P_a - P_T = 2P_r.$$

This error is tolerable for moderately low average SWR's (3 or less); for an average SWR of 3, the error is about 2 db. For better accuracy the power can be taken as the geometric mean of the maximum and minimum values of

$$P_p(P_a' = \sqrt{P_{p_{\max}} P_{p_{\min}}}).$$

This result will yield a maximum error of $2P_r$ and can also result in no error; the exact error is dependent on the phase ψ_{Mn} of each reflection coefficient.

VI. Conclusions

The fixed-probe technique using an oversize waveguide should be capable of accurately measuring multimode power up to at least the seventh harmonic of the band center for TE_{10} rectangular waveguide propagation. Experimental results indicate that agreement to better than ± 1 db is possible up to 3.5 times the fundamental frequency. The technique can accurately measure the power delivered to a mismatched load by using load reflection phase averaging in conjunction with a power measurement into a multimode matched load. Equipment is under development that will perform these measurements automatically. The theoretical analysis is presented for a rectangular waveguide but can also be extended to a coaxial line and other uniform transmission lines.

Appendix I

Power Flow in Rectangular Waveguide in Terms of Power Measured by Probes at the Boundary

An expression is derived for power flow in rectangular waveguide as a function of the power measured by electric probes located at the boundary of the guide in a plane transverse to the direction of propagation.

From the general theory of propagation in rectangular waveguide,

$$E_x = \sum_{m=0}^{M} \sum_{n=0}^{N} E_{mnx} \cos \frac{m\pi x}{a} \sin \frac{n\pi y}{b} \tag{11}$$

and

$$E_y = \sum_{m=0}^{M} \sum_{n=0}^{N} E_{mny} \sin \frac{m\pi x}{a} \cos \frac{n\pi y}{b} \tag{12}$$

where E_{mnx} and E_{mny} are the x and y components of the electric field of the mode whose indices are m, n. Substituting (11) and (12) into (3) yields

$$P = \frac{1}{\eta} \int_0^b \int_0^a \left[\left(\sum_{m=0}^{M} \sum_{n=0}^{N} E_{mnx} \cos \frac{m\pi x}{a} \sin \frac{n\pi y}{b} \right) \cdot \left(\sum_{m=0}^{M} \sum_{n=0}^{N} E_{mnx}^* \cos \frac{m\pi x}{a} \sin \frac{n\pi y}{b} \right) + \left(\sum_{m=0}^{M} \sum_{n=0}^{N} E_{mny} \sin \frac{m\pi x}{a} \cos \frac{n\pi y}{b} \right) \cdot \left(\sum_{m=0}^{M} \sum_{n=0}^{N} E_{mnx}^* \sin \frac{m\pi x}{a} \cos \frac{n\pi y}{b} \right) \right] dx dy. \tag{13}$$

When the integrations in (13) are carried out, the result is

$$P = \frac{ab}{2\eta} \left(\sum_{n=1}^{N} | E_{onx} |^2 + \sum_{m=1}^{M} | E_{moy} |^2 \right) + \frac{ab}{4\eta} \sum_{m=1}^{M} \sum_{n=1}^{N} (| E_{mnx} |^2 + | E_{mny} |^2). \tag{14}$$

The average of the power coupled by a large number of identical electric probes located on the periphery of a waveguide (Fig. 6) can be approximated by

$$P_p = \frac{ab}{2\eta\delta C} \left\{ \frac{1}{a} \int_0^a | E_y |_{y=0}^2 dx + \frac{1}{a} \int_0^a | E_y |_{y=b}^2 dx + \frac{1}{b} \int_0^b | E_x |_{x=0}^2 dy + \frac{1}{b} \int_0^b | E_x |_{x=a}^2 dy \right\} \tag{15}$$

where δ is a constant to be determined and where

E = rms electric field in the waveguide at a probe location,

E_p = rms electric field coupled by the probe, and

$$C = \frac{| E |^2}{| E_p |^2}.$$

When (11) and (36) are substituted in (15) and the integrations performed, the result is

$$P_p = \frac{ab}{4\eta\delta C}\left(\sum_{n=1}^{N} |E_{onx}|^2 + \sum_{m=1}^{M} |E_{moy}|^2\right) + \frac{ab}{4\eta\delta C}\sum_{n=1}^{N}\sum_{m=1}^{M}(|E_{mnx}|^2 + |E_{mny}|^2) + \frac{ab}{8\eta\delta C}\sum_{m=0}^{M}\left\{\sum_{n_2=0}^{N}\sum_{n_1=0}^{N} E_{mn_1y}E_{mn_2y}^*[1 + (-1)^{n_1+n_2}]\right\} + \frac{ab}{8\eta\delta C}\sum_{n=0}^{N}\left\{\sum_{m_1=0}^{M}\sum_{m_2=0}^{M} E_{m_1nx}E_{m_2nx}^*[1 + (-1)^{m_1+m_2}]\right\}. \quad (16)$$

A comparison of (14) and (16) shows that the first two terms of (16) are very similar to the power P in the waveguide. Disregarding the second two terms of (16) momentarily and defining

$$E' = \sum_{n=1}^{N} |E_{onx}|^2 + \sum_{m=1}^{M} |E_{moy}|^2 \quad (17)$$

$$E'' = \sum_{n=1}^{N}\sum_{m=1}^{M}(|E_{mnx}|^2 + |E_{mny}|^2) \quad (18)$$

the ratio of CP_p to P is

$$\frac{CP_p}{P} = \frac{\frac{1}{2\delta}(E' + E'')}{\left(E' + \frac{E''}{2}\right)}. \quad (19)$$

If E'' is zero (no power in modes with neither m nor n zero), the waveguide power P will be CP_p and $\delta = \frac{1}{2}$. If E' is zero (no power in modes with either m or n zero), the waveguide power will be CP_p and $\delta = 1$.

In general, the ratio of E'' to E' cannot be known exactly; however, a value of δ can be chosen that will minimize the error in

$$P = C_p P_p \quad (20)$$

where

$$C_p \equiv \delta_{\text{opt}} C.$$

This optimum value of δ, δ_{opt}, is chosen for the range of E''/E' that is expected in practice. If it is assumed that the range of E''/E' is from 0 to 2,

$$\delta_{\text{opt}} = 0.612. \quad (21)$$

Using this value for δ, the maximum error for the range from 0 to 2 is ± 0.88 db. A study of the modes launched by common coaxial-to-waveguide transitions is being undertaken. With this information it should be possible to reduce the error by optimizing δ for specific transitions and frequency ranges.

Data on the modal power distribution of two magnetrons is quoted in [9]. The first case is the third harmonic of an S-band magnetron, where E''/E' is 0.126. Using $\delta_{\text{opt}} = 0.612$, the error would be -0.63 db. The second case is the fifth harmonic of an L-band magnetron where E''/E' is 1.37. Using the same δ_{opt}, the error would be 0.60 db.

With (20) the first two terms of (16) can be identified as P/C_p, and (20) then becomes

$$P_p = \frac{P}{C_p} + \mathcal{E} \quad (22)$$

where $\mathcal{E}$ represents the remaining terms in (16). The terms in $\mathcal{E}$ are error terms, since they cause the power computed from (20) to differ from the waveguide power.

The first error term is

$$\mathcal{E}_1 = |E_{01x}|\,|E_{21x}|\cos[\phi_1 + (\beta_{21} - \beta_{01})l] \quad (23)$$

where

ϕ_1 = initial phase difference between E_{01x} and E_{21x}

β_{01}, β_{21} = phase constants of the 0, 1 and 2, 1 modes

l = length of S-band waveguide.

The cutoff frequency of the 2,1 mode in S-band waveguide is 6.06 Gc. Hence, below this frequency $\mathcal{E}$ is zero and (20) can be used directly to compute the waveguide power from a single measurement of P_p. Above 6.06 Gc the 0,1 and 2.1 modes can exist in S-band waveguide. If the transmitting tube-to-waveguide transition launches these modes, $\mathcal{E}_1$ will not be zero. However, since $\mathcal{E}$ is the only term in (22) that depends on l, $\mathcal{E}_1$ can be made to cancel. If a line stretcher in the S-band waveguide (which is dispersive) is adjusted to obtain the maximum and minimum values of P_p, the result is

$$P_{p\max} = \frac{P}{C_p} + \mathcal{E}_1 \quad (24)$$

$$P_{p\min} = \frac{P}{C_p} - \mathcal{E}_1. \quad (25)$$

Averaging these two equations causes $\mathcal{E}_1$ to cancel and the result is (20), where P_p is now interpreted as the peak-to-dip average $(P_{p\max} + P_{p\min})/2$.

Above 7.65 Gc, the second error term

$$\mathcal{E}_2 = |E_{11x}|\,|E_{31x}|\cos[\phi_2 + (\beta_{31} - \beta_{11})l] \quad (26)$$

can exist in the S-band waveguide. At 10 Gc it is possible to have seven error terms. However, in a practical measurement, it is unlikely that all of them will have sufficient amplitude to cause an appreciable error. In particular, modes whose m indices are even will not be launched by symmetrical coaxial-to-waveguide transitions that are located in the center of the broad wall of the waveguide. Furthermore, modes that are close to their cutoff frequency are difficult to launch [9]. For these reasons it is believed that, in practice, one error term will be dominant, and the use of the line stretcher to obtain the peak-to-dip average will result in accurate power measurements.

Appendix II

Power Flow in Multimode Rectangular Waveguide

This appendix derives the expression for the total incident power flowing in an enlarged rectangular waveguide containing an arbitrary set of TE and TM modes coupled to it from a standard size waveguide. Total power is obtained from integration of the Poynting vector. The result is expressed in terms of a simplified but approximate formula. Estimates of the error resulting from its use are given.

The coordinate system is shown in Fig. 6. The time-average power flow in the z direction is given by

$$P = \int_0^b \int_0^a [\mathrm{Re}\, \overline{E} \times \overline{H}^*] \cdot \bar{z} dxdy \tag{27}$$

where $\overline{E}$ and $\overline{H}$ are the rms values of the electric and magnetic fields, respectively, and $\bar{z}$ is a unit vector in the $\bar{z}$ direction.

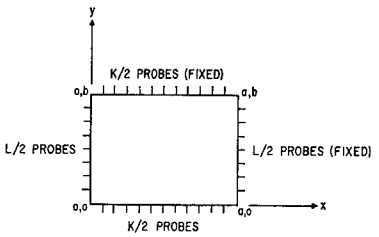

Fig. 6—Cross section of enlarged waveguide with fixed-probes.

Expanding the fields into their components gives the following simplification to (27):

$$P = \int_0^b \int_0^a \mathrm{Re}\, (E_x H_y^* - E_y H_x^*) dxdy. \tag{28}$$

To determine P in a waveguide propagating two or more modes from (28), the magnitudes and phases of E_x, H_y, E_y and H_x would have to be known over the entire cross section. If the waveguide containing these modes is tapered into an enlarged guide, the cutoff frequencies of all propagating modes will be much less than the applied frequency; the oversize guide wavelength λ_g approaches the free space wavelength λ. This causes the wave impedances Z_w, for all TM and TE modes to approach η, the intrinsic impedance of free space. By noting that

$$Z_w = \frac{E_x}{H_y} = -\frac{E_y}{H_x}. \tag{29}$$

Eq. (28) becomes

$$P = \frac{1}{\eta} \int_0^b \int_0^a (|E_x|^2 + |E_y|^2) dxdy. \tag{30}$$

Thus, P can be determined in the enlarged guide from only the magnitude of E_x and E_y over the cross section of the oversize waveguide.

Eq. (29) is exact only for a and b approaching ∞. We wish to estimate the error for practical enlarged waveguide, *i.e.*, three times the size of a standard guide in both a and b dimensions. The maximum possible error would occur when all the power exists in a mode just slightly above cutoff in the standard guide. By computing this power and comparing it with (29), the error can be estimated. This error will be an upper bound because all other modes will be further away from cutoff (closer to a plane-wave condition). For this single mode case, the power flow P is determined by substituting (29) in (28) giving

$$P' = \frac{1}{Z_w} \int_0^b \int_0^a (|E_x|^2 + |E_y|^2) dxdy \tag{31}$$

where

$$Z_w = \eta \frac{\lambda_g}{\lambda} \qquad \text{for a TE mode}$$

and

$$Z_w = \eta \frac{\lambda}{\lambda_g} \qquad \text{for a TM mode.}$$

The error in P' due to using (30) is therefore

$$\epsilon = \frac{P - P'}{P'} = \frac{Z_w}{\eta} - 1. \tag{32}$$

For the TE mode case the error is

$$\epsilon_{TE} = \frac{\lambda_g}{\lambda} - 1 = \left[1 - \left(\frac{f_c}{f}\right)^2\right]^{-1/2} - 1$$

$$\approx \frac{1}{2}\left(\frac{f_c}{f}\right)^2 \qquad \text{for } \frac{f_c}{f} \ll 1 \tag{33}$$

and for the TM mode the error is

$$\epsilon_{TM} = \frac{\lambda}{\lambda_g} - 1 = \left[1 - \left(\frac{f_c}{f}\right)^2\right]^{1/2} - 1$$

$$\approx -\frac{1}{2}\left(\frac{f_c}{f}\right)^2 \qquad \text{for } \frac{f_c}{f} \ll 1. \tag{34}$$

We can now evaluate the error for guide three times the size of standard guide. The maximum error occurs when $f_c/f = \frac{1}{3}$. Subsitution of $f_c/f = \frac{1}{3}$ in either (33) or (34) predicts an error of 6 per cent.

Appendix III

Evaluation of Fixed-Probe Error Terms for the Third Harmonic

We wish to determine the error in using the fixed-probe method for measuring the third harmonic of an S-band signal in the range of 3.2 to 3.4 Gc. Fig. 1(a) (S-band) indicates that, for third-harmonic frequencies, modes having the following mn indices can propagate in S-band waveguide: 10, 20, 01, 11, 21, 22, 30, 31, 40, 41.

Subsituting the indicated E_{mn} values in the error terms of (16) and excluding all terms having E_{0n_y} and E_{m0_x} (these field components do not exist), we obtain

$$\mathcal{E}_y = \frac{ab}{2\eta\delta C} \operatorname{Re} (E_{10_y}E_{12_y}^* + E_{20_y}E_{22_y}^*)$$

and

$$\mathcal{E}_x = \frac{ab}{2\eta\delta C} \operatorname{Re} (E_{01_x}E_{21_x}^* + E_{02_x}E_{22_x}^* + E_{01_x}E_{41_x}^* + E_{11_x}E_{31_x}^* + E_{21_x}E_{41}^*) \quad (35)$$

where $\mathcal{E}_y$ is the power error due to E_y fields, and $\mathcal{E}_x$ is the error due to E_x fields.

For the special case of a symmetrical transition from the transmitter to the waveguide with respect to the x dimension, the error terms simplify because all terms having an even m index will not exist. The simplified expressions are

$$\mathcal{E}_y = \frac{ab}{2\eta\delta C} \operatorname{Re} E_{10_y}E_{12_y}^*$$

and

$$\mathcal{E}_x = \frac{ab}{2\eta\delta C} \operatorname{Re} E_{11_x}E_{31_x}^* \quad (36)$$

Acknowledgment

The author wishes to thank the following Airborne Instruments Laboratory personnel: J. Goldberg, O. Hinckelmann, and R. Sleven for helpful comments, and H. Franck and D. Levinson for performing the measurements. The suggestion of geometric mean power averaging (Section V) was due to S. Cohn of Armour Research Foundation.

Bibliography

[1] M. P. Forrer and K. Tomiyasu, "Effects and measurements of harmonics in high power waveguide systems," 1957 IRE National Convention Record, pt. 1, pp. 263–269.

[2] V. G. Price, "Measurement of harmonic power generated by microwave transmitters," IRE Trans. on Microwave Theory and Techniques, vol. MTT-7, pp. 116–120; January, 1959.

[3] D. J. Lewis, "Mode couplers and multimode measurement techniques," IRE Trans. on Microwave Theory and Techniques, vol. MTT-7, pp. 110–116; January, 1959.

[4] E. D. Sharp and E. M. T. Jones, "A sampling measurement of multimode waveguide power," IRE Trans. on Microwave Theory and Techniques, vol. MTT-10, pp. 73–82; January, 1962.

[5] J. Goldberg, O. Hinckelmann, D. Levinson, R. Sleven and J. Taub, "Second Quarterly Progress Report on New Methods for Measuring Spurious Emissions," Airborne Instruments Lab., Div. of Cutler-Hammer Inc., Deer Park, N. Y., Rept. No. 1112-I-2, AF 30(602)-2511; November, 1961.

[6] H. G. Unger, "Circular waveguide taper of improved design," *Bell Sys. Tech. J.*, vol. 37, pp. 899–912; July, 1958.

[7] C. C. H. Tang, "Optimization of waveguide tapers capable of multimode propagation," IRE Trans. on Microwave Theory and Techniques, vol. MTT-9, pp. 442–452; September, 1961.

[8] O. Hinckelmann, R. Sleven and L. Moses, "Equipment for the measurement of spurious emissions," *Symp.* IRE Professional Group on Radio Frequency Interference, San Francisco, Calif.; June, 1962.

[9] V. G. Price, J. P. Rooney and C. Milazzo, "Final Report: Phase I—Measurement and Control of Harmonic and Spurious Microwave Energy," G. E. Microwave Lab., Palo Alto, Calif. Rept. [T1SR58 ELM 112, AF 30(602)-1670; July 8, 1958.

[10] J. Goldberg, O. Hinckelmann, D. Levinson, R. Sleven and J. Taub, "First Quarterly Progress Report on New Methods, for Measuring Spurious Emissions," Airborne Instruments Lab., Div. of Cutler-Hammer Inc., Deer Park, N. Y., Rept. No. 1112-I-1, AF 30(602)-2511; August, 1961.

[11] N. Marcuvitz, "Waveguide Handbook," MIT Radiation Laboratory Series, McGraw-Hill Book Co., Inc., New York, N. Y., vol. 10, p. 57; 1951.